A Scalable Low-Cost-UAV Traffic Network (uNet)

Santosh Devasia[a] and Alexander Lee[b]
U. of Washington, Seattle, WA 91895-2600

This article proposes a new Unmanned Aerial Vehicle (UAV) operation paradigm to enable a large number of relatively low-cost UAVs to fly beyond-line-of-sight (BLOS), without costly sensing and communication systems or substantial human intervention in individual UAV control, in UAV-only traffic that is separated from non-UAV airspace. The main contribution of this work is to propose the use of pre-established route network for UAV traffic management, which allows: (i) pre-mapping of obstacles along the route network to reduce the onboard sensing requirements and the associated costs for avoiding such obstacles; and (ii) use of well-developed routing algorithms to select UAV schedules that avoid UAV-UAV conflicts. Available GPS-based navigation can be used to fly the UAV along the selected route and time schedule with relatively low added cost, which therefore, reduces the barrier to entry into new UAV-applications market. Additionally, this article proposes a new decoupling scheme for conflict-free transitions between edges of the route network at each node of the route network to reduce potential conflicts between UAVs and ensuing delays. A simulation example is used to illustrate the proposed uNet approach.

[a] Professor, Mechanical Engineering Dept., Box 352600, AIAA Senior Member.
[b] Volunteer Student, Mechanical Engineering Dept., Box 352600.

I. Introduction

This article proposes a new Unmanned Aerial Vehicle (UAV) operation paradigm to enable a large number of relatively low-cost UAVs to fly beyond-line-of-sight, without costly sensing and communication systems or substantial human intervention in the individual UAV control. A broadly accessible UAV traffic network (uNet) for low-cost UAVs can reduce the barrier to entry into the UAV market and enable new commercial enterprises and applications. For example, just as mobile phones revolutionized communication in developing countries by circumventing costly landlines, minimalist UAVs could make product delivery a reality in geographic areas where transportation infrastructure is difficult and prohibitively expensive to build. The uNet itself can be an agglomeration of new franchise operators, along with internet-based application (APP) providers who enable users to automatically negotiate between different operators, and get a UAV to its destination. Additionally, existing commercial delivery companies can use the uNet to transport products and smaller UAV brokerage firms can use it to transport UAVs between locations.

Under the current free-flight-like paradigm, the initial UAV route selection only needs to avoid restricted airspace and altitudes without considering the pre-scheduled routes of other UAVs and intent of other users. Such freedom to fly anywhere, nevertheless, creates challenges when trying to avoid obstacles and collisions with potentially other UAVs. Additionally, without a-priori detailed information of the entire airspace, the free-flight approach leads to lack of knowledge about the immediate surroundings of the UAV, which then requires sensors and/or humans to detect obstacles. Moreover, the UAV could have potential conflicts with other UAVs and obstacles along the way, which in turn, requires expensive on-board sensing and communication as well as substantial human effort. The ultimate consequence of this is an increased cost of UAV operation, scaling upwards in complexity as more and more UAVs are introduced. Conflict resolution protocols in the free-flight system would need to continually evolve as density increases, and sensors and UAV-to-UAV communications would need to become progressively more sophisticated, e.g., for potential collaborative conflict resolution, as investigated previously for manned aircraft [29, 30]. An approach that can avoid the increased complexity and cost of UAV-to-UAV communication is to develop pre-specified conflict avoidance rules for UAVs that are similar to visual flight rules (VFR) for manned aircraft.

However, it can be challenging to develop such VFR rules that are provably safe with a large number of UAVs with multiple independent UAV operators. Another approach is to use human-guided conflict resolution similar to current air traffic management (ATM) for commercial manned flights over controlled airspace [31–34]. The human effort required for such conflict resolution can be lessened by using emerging concepts such as sense and avoid [35]. Nevertheless, the human workload for conflict detection and avoidance tends to increase with number of aircraft, which limits the ability to scale such human-centered methods for a large number of UAVs. The increased cost, of the UAV and its operation, also serves as an impediment to the emergence and development of broader UAV applications.

The new idea proposed here is to place the UAVs along an established route network, similar to automated guided vehicles on a factory floor [36, 37], or the jet routes followed by commercial aircraft in controlled airspace [38]. These routes can be dense and time-varying to optimize for and accommodate conditions such as wind speed, precipitation, and other potential local variables. Routes could be ad-hoc networks set up to meet application requirements, e.g., for agricultural applications or coordinated disaster relief. Even with a high density of UAVs in flight, such route networks can provide sufficient flexibility while also addressing privacy concerns. A UAV using this route network could get to a typical home by flying over conventional roads, without flying over private property or other restricted areas.

Compared to the free-flight-style of UAV traffic management, the proposed approach over established route networks (such as roadways) offers two major advantages. First, obstacles along the routes can be mapped a-priori and updated as needed, reducing onboard sensing requirements. Note that detailed mapping of obstacles is only needed along the routes in this approach and not the entire airspace as in the free-flight approach. Waypoints along these established routes can be used to fly the UAV along a three dimensional trajectory, e.g., [39, 40]. The management of initial and final departure by an expert human, say for arrival to or departure from a supermarket, will increase the operational cost of the system. An alternative is to use automated approaches such as GPS-based landing schemes, e.g., [41, 42]. Then, for UAV traffic management, the amount of sensing and data required on each UAV reduces to GPS-enabled navigation from a given waypoint

to the next specified waypoint. The low cost of GPS-based navigation can reduce the barrier to entry into new UAV-applications market. For example, an Insitu ScanEagle system with four air vehicles, a ground control station, remote video terminal, the launch system and recovery system costs about $3 million. In contrast, a hobby-type UAV with GPS-based navigation system is about three orders of magnitude lower in cost. Moreover, since the proposed approach does not require active imaging and sensing of the surroundings, such an approach could alleviate some of the privacy concerns associated with UAVs with substantial sensing capabilities.

A second advantage is that conflict resolution over a route network can be transformed into a re-source allocation problem, i.e., two UAVs cannot occupy the same section of a route at the same time. Additionally, transitions between different sections of the network can be designed to be conflict-free for reducing potential delays, e.g., [43]. Then, conflict-free route selection can be solved using well-developed existing resource allocation procedures for multi-agent systems, e.g., [36, 37, 44–48]. For example, scheduling can be done using context-aware route planning (CARP), where a new agent (i.e., the UAV) selects a route from a route network (e.g., selects a shortest path-length route [49]) and schedules the arrival time such that the new agent is conflict-free with respect to pre-vious agents that have been scheduled already [44]. As opposed to the computationally-challenging, simultaneous optimization over all agents to find conflict-free routing problems, CARP finds less optimal solutions by using a first come first served (FCFS) approach. Although not optimal such FCFS approaches are typically considered fair, e.g., in conventional Air Traffic Management [33]. In such a scenario, simultaneous conflicting requests could be sequenced randomly, which would also be considered as an unbiased solution when all other things are equal. The proposed a-priori de-conflicting using scheduling reduces the amount of on-board sensing and communication needed on each UAV. Thereby, the proposed uNet enables access to low-cost UAV, and consequently can lead to broad usage of the uNet.

Another contribution of this work is to propose a new decoupling scheme for conflict-free tran-sitions between edges of the route network at each node of the route network to reduce potential conflicts between UAVs. At low UAV densities, establishing a waiting protocol at nodes of the route network could be one possible method of conflict avoidance. Unfortunately, this method incurs

additional fuel costs to slow down from cruise and hover, and then accelerate again. If the conflicts at the nodes can be avoided by design, such delays can be reduced or even eliminated entirely. This is similar to the design of multi-level interchanges at freeway junctions that allow multiple traffic streams to pass through without crossing each other as opposed to the use of traffic lights or stop signs on typical surface streets.

In addition to offering solutions for prior waypoint mapping and conflict resolution, the uNet approach is also capable of distributed development and implementation through sector-level uNets (sNets) that each manage UAVs inside their local region of the airspace. With minimal effort from the user, who only needs to specify initial and final locations along with an estimated time of arrival (ETA), a service, possibly a commercial web-application (APP), can select a route that spans multiple sNets and choose a scheduled time of arrival (STA) into the uNet based on route-availability. The APP serves to negotiate between different sNets and manage different service fees and availability along en-route sNets to propose a scheduled time of arrival (STA) into the uNet. If the UAV meets requirements such as fuel for the flight, GPS and communication needs between the UAV and sNets, and human-guided (or automated) initial and final transitions into and out of the uNet, then the flight is accepted into the first sNet. Communication between the sNet and a UAV, e.g., about waypoint specifications and current location updates (using GPS on the UAV), can be done using cellular data. This allows each sNet to manage and monitor UAV flights and conflict avoidance in its airspace. In case of emergencies which is another important issue in beyond line of sight operation, e.g., [50], the sNet can potentially redirect the UAV by providing new waypoints that could be precomputed for every section of the route network. Moreover, each sNet will keep track of route occupancy (resource allocation) in its airspace and dynamically update the available route network if needed.

The proposed distributed approach allows public-private partnerships to manage different aspects of the uNet such as management and regulation of the sNets. A progressive rollout and expansion of the uNet infrastructure, one sNet piece at a time, can enable organic growth of the overall uNet. Commercial groups (such as local supermarkets or malls) can develop and manage the local sNets, and sNets can be either refined over time into smaller sectors with a finer mesh or

integrated together to form larger sectors. Similar to the development of the National Science Foundation (NSF) NSFNET, which provided the backbone communication service for the Internet, the public sector could help the uNet effort by developing backbone-type services, e.g., over highways to connect local sNets.

The article begins with a description of the proposed uNet structure in Section II and then presents the de-conflicting scheme in Section III. The resource-allocation approach to UAV scheduling is illustrated with a simulation example in Section IV, which is followed by conclusions.

II.   Proposed uNet structure

A.   UAV routing through sNets

The uNet consists of multiple sector-level uNets (sNets), each of which controls a specified region of the airspace. After entering a desired initial location L_i in the initial sNet $S_k(1)$, a UAV U can potentially transition through multiple such sNets before reaching the final location L_f in the final sNet $S_k(n_{s,k})$ as illustrated in Fig. 1. For a given expected time of arrival ETA(k) into the uNet, the router negotiates between multiple sNets to determine the scheduled time of arrival STA(k) and a conflict-free flight route $R(k)$ that spans multiple sNets $\{S_k(i)\}_{i=1}^{n_{s,k}}$. The UAV $U(k)$ receives GPS information and communicates its position $P[U(k)](t)$ to the current sNet $S_k(i)$ at time t.
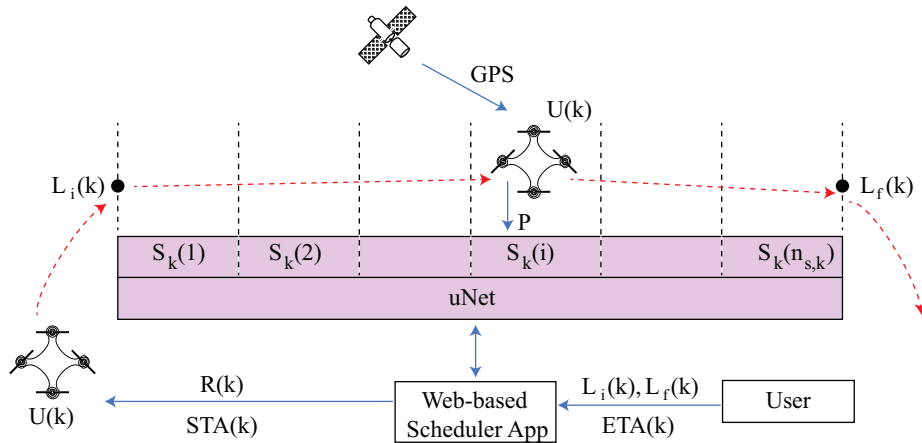

Fig. 1 Schematic routing of the kth UAV $U(k)$.

In particular, given the expected time of arrival ETA(k) of the kth UAV $U(k)$ into the initial location $L_i(k)$ and the final location $L_f(k)$, a router (potentially a web-based application) negotiates

6

between multiple sNets to determine a scheduled time of arrival STA(k) and a flight route $R(k)$ that is conflict-free with respect to all the prior UAVs $[U(i)]_{i=1}^{k-1}$ in the uNet.

B. Definition: conflict-free

In the following, two UAVs $U(i)$ and $U(j)$ are considered to be in conflict at some time t if they are inside the uNet region and their minimal separation is less than an acceptable value d_{sep}, i.e.,

$$\|L[U(i)](t) - L[U(j)](t)\|_2 < d_{sep} \tag{1}$$

where $\|\cdot\|_2$ is the standard Euclidean norm and $L[U(\cdot)](t)$ is the position of the UAV $U(\cdot)$ at time t. The minimal separation d_{sep} is needed to ensure that there are no collisions with other UAVs, even with potential errors in UAV positioning. Thus, the minimal separation d_{sep} between UAVs, needed to be be conflict-free, will depend on the precision of the GPS-based navigation system.

The routes are selected by the local sNets to be obstacle free. Enroute sNets $[S_k(i)]_{i=1}^{n_{s,k}}$ ensure that all routes including the selected route $R(k)$ for the UAV $U(k)$ are clear of obstacles in each sNet $S_k(i) \in \mathcal{S}$ that the kth UAV $U(k)$ passes through where $\mathcal{S}$ is the set of sNets and $n_{s,k}$ is the number of sNets traversed as in Fig. 1. The flight route $R(k)$ can be used to determine the fuel required for the flight. If the UAV meets the previously-specified requirements for flight (e.g., amount of fuel), then the flight is accepted by the first sNet $S_k(1)$ on the selected flight route $R(k)$.

C. Specified route structure

Under a specified route structure scenario, the potential route R of a UAV U can be selected from edges of a directed graph $\mathcal{G} = (\mathcal{N}, \mathcal{E})$ with nodes $\mathcal{N}$ enumerated as $[N(i)]_{i=1}^{n_n}$, $n_n > 1$ and edges $\mathcal{E} \subseteq \mathcal{N} \times \mathcal{N}$ enumerated as $[E(j)]_{j=1}^{n_e}$, $n_e \geq 1$. There is a path on the graph from every desired initial location to every desired final location. It is assumed that each node in the uNet has a distinct spatial location, and the edges connect distinct points in space. Therefore, the initial node $N([j]_i)$ and the final node $N([j]_f)$ of each edge $E_j = \{N([j]_i), N([j]_f)\} \in \mathcal{E}$ are different, i.e., $N([j]_i) \neq N([j]_f)$.

Remark 1 (General 3-dimensional edges) *The edges $\mathcal{E}$ between nodes in the graph $\mathcal{G}$ could be general curved paths and can be three dimensional. Alternatively, general curved paths could be*

approximated with straight-line segments and the start and end of these segments could be included in the set of graph nodes $\mathcal{N}$.

Given an initial node $L_i(k)$ and final node $L_f(k)$ for the kth UAV $U(k)$, a route $R(k)$ is a path on the graph $\mathcal{G}$, i.e., sequence of distinct edges,

$$R_k = [E_k(1),\ E_k(2),\ \ldots,\ E_k(n_{r,k})],\quad \text{where } E_k(j) = \{N_k([j]_i), N_k([j]_f)\} \in \mathcal{E}, \tag{2}$$

$n_{r,k}$ is the number of edges in route R_k, with a sequence of distinct nodes

$$N(R_k) = [L_i(k),\ N_k([1]_f),\ N_k([2]_f),\ \ldots,\ N_k([n_{r,k}]_f)]. \tag{3}$$

Therefore, the edges are connected, i.e., initial nodes $N_k([\cdot]_i) \in \mathcal{N}$ and final nodes $N_k([\cdot]_f) \in \mathcal{N}$ satisfy

$$N_k([j]_f) = N_k([j+1]_i),\quad \forall j = 1, 2, \ldots, (n_{r,k} - 1), \tag{4}$$

without retracing an edge, i.e.,

$$N_k([j]_i) \neq N_k([j+1]_f),\quad \forall j = 1, 2, \ldots, (n_{r,k} - 1), \tag{5}$$

and the edges begin and end at the desired initial and final locations, i.e.,

$$N_k([1]_i) = L_i(k),\quad N_k([n_{r,k}]_f) = L_f(k) \tag{6}$$

D.   sNets

The uNet is partitioned into n_s number of sNets $\mathcal{S} = [S(j)]_{j=1}^{n_s}$ such that each edge inside the set of edges $\mathcal{E}$ of the uNet graph $\mathcal{G}$ belongs to a unique sNet. Each sNet $S(i)$ can be considered as a subgraph $\mathcal{G}_i = (\mathcal{N}_i, \mathcal{E}_i)$ of the overall graph $\mathcal{G}$ with $\mathcal{N}_i \subseteq \mathcal{N}$ and $\mathcal{E}_i \subseteq \mathcal{E}$. An example sNet $S(1)$ is shown in Fig. 2, where the set of nodes $\mathcal{N}_1 \subseteq \mathcal{N}$ associated with the sNet

$$\mathcal{N}_1 = [N_1(1),\ N_1(2),\ \ldots,\ N_1(12)] \tag{7}$$

is represented by numbered dots $[i]_{i=1}^{12}$ on a square gird with the same vertical height and the set of edges

$$\mathcal{E}_1 \subseteq (\mathcal{N}_1 \times \mathcal{N}_1) \cap \mathcal{E} \tag{8}$$

associated with the sNet is enumerated as $[E_1(i)]_{i=1}^{26}$ and given by

$$
\mathcal{E}_1 = \begin{bmatrix} \{1,4\}, \{2,5\}, \{3,4\}, \{4,1\}, \{4,3\}, \{4,5\}, \{4,7\}, \{4,8\}, \{5,2\}, \{5,4\}, \\ \{5,6\}, \{5,9\}, \{6,5\}, \{7,4\}, \{8,4\}, \{8,9\}, \{8,11\}, \{9,5\}, \{9,8\}, \{9,10\}, \\ \{10,9\}, \{10,11\}, \{11,8\}, \{11,10\}, \{11,12\}, \{12,11\} \end{bmatrix}.
\tag{9}
$$

Note that the example sNet $S(1)$ includes typical roadway intersection geometries such as T-intersection at node 9, Y-intersection at node 8, cross-intersection at node 5, and a general non-circular intersection with more than four legs at node 4. Note that the T and Y intersections are operationally similar, i.e., 3-way intersections, although it is possible to develop algorithms that provide priority to the straight segments of a T intersection, e.g., by having smaller number of turns.
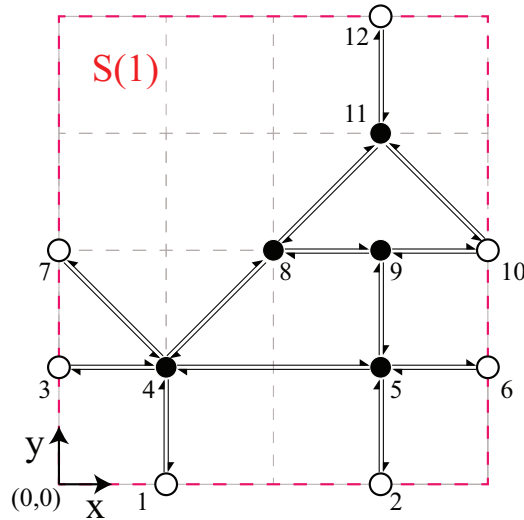
Fig. 2 Example sNet $S(1)$ with typical roadway intersections.

III.   De-conflicting UAV routes

Potential conflicts between two UAVs on two routes are classified into two scenarios: (i) when the two routes do not share an edge; and (ii) when the two routes share an edge. De-conflicting UAV routes without a shared edge is discussed next and the second scenario where routes share an edge is discussed in subsection III B.

A. Scenario 1: de-conflicting UAV routes without shared edge

It is assumed in the following that the uNet design is such that edges are sufficiently spaced from each other to avoid conflicts between two UAVs on two distinct routes that do not share any edges, especially far away from common nodes, as stated formally below.

Assumption 1 (Sufficiently-spaced edges) *The overall uNet graph $\mathcal{G}$ is constructed (with edges sufficiently spaced from each other) such that two UAVs one on each of two distinct edges, say $E(i)$ and $E(j)$, cannot have conflicts if the two edges do not have a node N in common.*

Assumption 2 (Conflict-free away from nodes) *If two distinct edges $E(i)$ and $E(j)$ have a common node N, then there is no conflict between two UAVs (one UAV on each of these two edges), when at least one of the UAVs is not inside a vertical conflict-free boundary cylinder of radius $d^*[N]$*

$$d^*[N] \geq d_{sep} \tag{10}$$

*centered around the common node N and height $h^*[N]$.*

Assumption 3 (Edges planar near nodes) *In the following, it is assumed that for each node N in the uNet graph $\mathcal{G}$, each of the n_N edges, say $E_N(i)$, in the set of edges $\mathcal{E}_N = [E_N(j)]_{j=1}^{n_N}$ connected to the node N intersects with the conflict-free boundary cylinder (in Assumption 2) at a single point $a_N(i)$. Moreover, the set of intersection points $\mathcal{A}_N = [a_N(i)]_{i=1}^{n_N}$ for each node N lie on a single horizontal plane, on a conflict-free boundary circle $B_c[N] \subseteq B_s[N]$.*

Assumptions 2 and 3 imply that all the edge-intersection points in the set $\mathcal{A}_N$ on the circumference of the conflict-free boundary circle $B_c[N]$ of a node N are sufficiently separated, i.e.,

$$d(\mathcal{A}_N) \quad = \min_{i \neq j} \left\{ d(N_i, N_j) \mid N_i \in \mathcal{A}_N, N_j \in \mathcal{A}_N \right\} \quad \geq d_{sep}. \tag{11}$$

Nevertheless, two UAVs $U(i)$ and $U(j)$ on routes R_i and R_j respectively that share no edges could encounter conflict as they approach a shared node N, i.e., $N \in \{P(R_i) \cap P(R_j)\}$ where the set of nodes of a route $P(\cdot)$ is defined in Eq. 3. To illustrate, in the example sNet $S(1)$ in Fig. 2, a UAV, say $U(1)$ on route $R(1)$ from node 8 to node 10 that includes a transition from edge $\{8, 9\}$ to edge $\{9, 10\}$ in Fig. 3(a) could have a conflict near the common node 9 with a UAV, say $U(2)$ on route

$R(2)$ from node 10 to node 5 that includes a transition from edge $\{10,9\}$ to edge $\{9,5\}$. When both UAVs are inside the space circumscribed by the boundary circle $B_c[9]$ shown in Fig. 3(b) that is centered around node 9, the potential for conflict needs to be anticipated and resolved.

(a) Node N=9

(b) Zoomed view of boundary circle

(c) Three-level transition
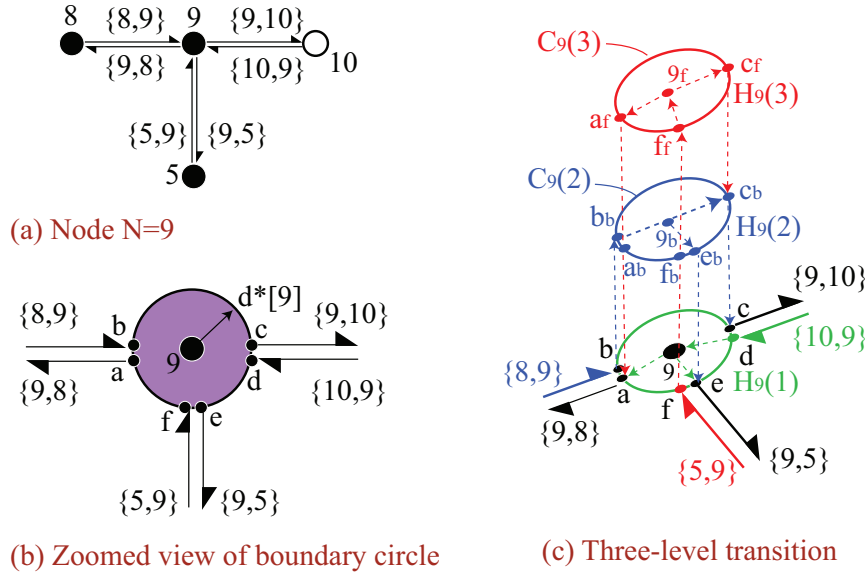
Fig. 3 Example decoupled edge-to-edge transitions at node 9 of sNet $S(1)$ in Fig. 2.

Potential conflicts, between UAVs on routes that do not share an edge but share a common node as described above, can be avoided by sufficiently separating the transitions between edges at all nodes. To achieve this separation, the transitions from each edge in the set of edges $\underline{\mathcal{E}}_N = [\underline{E}_N(j)]_{j=1}^{n_N}$ into a node N to an edge in the set of edges $\overline{\mathcal{E}}_N = \left[\overline{E}_N(j)\right]_{j=1}^{\overline{n}_N}$ out of the same node N are accomplished at different-height levels $\mathcal{H}_N = [H_N(j)]_{j=1}^{n_N}$. Each level, e.g., $H_N(i)$ is a horizontal plane separated from all other levels by at least height h_N. Let the UAV be transitioning from edge, say $\underline{E}_N(i) \in \underline{\mathcal{E}}_N$, into node N to edge, say $\overline{E}_N(j) \in \overline{\mathcal{E}}_N$, out of node N. Moreover, let the intersections of these edges $\underline{E}_N(i)$ and $\overline{E}_N(j)$ with the the conflict-free boundary circle $B_c[N]$ (in Assumption 3) be $\underline{a}_N(i)$ and $\overline{a}_N(j)$, respectively. Once the UAV on edge $E_N(i)$ reaches $\underline{a}_N(i)$ at the edge of the conflict-free boundary circle $B_c[N]$, the UAV moves vertically to the ith level $H_N(i)$, then horizontally on this level $L_N(i)$ to be located directly above node N before moving horizontally towards the location on level i that is directly above $\overline{a}_N(j)$. Then, the UAV descends vertically down from level $H_N(i)$ to $\overline{a}_N(j)$ at the edge of the conflict-free boundary circle $B_c[N]$ and moves out of node N along the edge $\overline{E}_N(j)$.

Remark 2 (Transition levels above and below node) *The levels associated with the edge-transitions of a node N need not be all above the node, they can be below or at the same height as the node N provided such spaces are free of nodes, edges, obstacles, or other constraints preventing use by the UAV.*

To illustrate the de-conflicted edge transitions, consider the node $N = 9$ in the example sNet $S(1)$, which has six edges,

$$
\begin{aligned}
\mathcal{E}_9 &= [E_9(1),\ E_9(2),\ E_9(3),\ E_9(4),\ E_9(5),\ E_9(6)] \\
&= [\{10,9\},\ \{8,9\},\ \{5,9\},\ \{9,10\},\ \{9,8\},\ \{9,5\}]
\end{aligned}
\tag{12}
$$

connected to the node, where three of these edges,

$$
\underline{\mathcal{E}}_9 = [\underline{E}_9(1),\ \underline{E}_9(2),\ \underline{E}_9(3)] = [\{10,9\},\ \{8,9\},\ \{5,9\}]
\tag{13}
$$

are into node $N = 9$, as shown in Fig. 3(a). Therefore, three levels $\mathcal{H}_9 = [H_9(j)]_{j=1}^3$ (at different heights) are used for transitions from each of the edges in $\underline{\mathcal{E}}_9$ into the node $N = 9$ to the output edges

$$
\overline{\mathcal{E}}_9 = [\overline{E}_9(1),\ \overline{E}_9(2),\ \overline{E}_9(3)] = [\{9,10\},\ \{9,8\},\ \{9,5\}]
\tag{14}
$$

out of node $N = 9$, as illustrated in Fig. 3(c). Let a UAV aim to transition from edge $\underline{E}_9(2) = \{8,9\}$ into node $N = 9$ to edge $\overline{E}_9(3) = \{9,5\}$ out of node $N = 9$. Moreover, let the intersections of these edges $\underline{E}_9(2)$ and $\overline{E}_9(2)$ with the the conflict-free boundary circle $B_c[N]$ (in Assumption 3) be $\underline{a}_9(2) = b$ and $\overline{a}_9(2) = e$, respectively, as in Fig. 3(c). Once the UAV on edge $\underline{E}_9(2) = \{8,9\}$ reaches $\underline{a}_9(2) = b$ on the circumference of the conflict-free boundary circle $B_c[9]$, the UAV moves vertically to the 2nd level $H_9(2)$, then horizontally on this level, $H_9(2)$ to be located at 9_b directly above node $N = 9$ before moving horizontally towards the location e_b on level $H_9(2)$ that is directly above the location $\overline{a}_9(2) = e$. Then, the UAV descends vertically down from level $H_9(2)$ to location $\overline{a}_9(2) = e$ on the circumference of the conflict-free boundary circle $B_c[9]$ and moves out of node $N = 9$ along the edge $\overline{E}_N(j) = \{9,5\}$.

Remark 3 (Avoid back tracking) *Since the nodes in a route $(P(\cdot)$ defined in Eq. 3) are distinct, transitions to edges that return back to the start node of an edge into a node are not needed, e.g.,*

transition from edge $\{8,9\} \in \underline{\mathcal{E}}_9$ to edge $\{9,8\} \in \overline{\mathcal{E}}_9$ is not needed at node $N = 9$, and is therefore, not shown in Fig. 3(c).

Even with the multiple-level edge-to-edge transitions at a common node N, the minimal distance between two UAVs on two different routes $R(i)$ and $R(j)$ without a common edge can be made larger than the acceptable value d_{sep} to avoid conflicts. Note that, from Assumptions 1-3, conflicts cannot occur on the edges if both UAVs are outside the conflict-free boundary circle $B_c[N]$ of a common node, say N. The UAVs have to arrive into the node N through different edges since their associated routes do not share a common edge, and therefore, are designed to achieve edge-transitions using different levels in the proposed scheme. Moreover, since the input and output edges from the node N are different, the two UAVs also do not share the vertical ascending and descending paths.

There are three possible cases under which a conflict can occur between two UAVs:

1. both UAVs are on the ascending or descending paths to different edge-to-edge transition levels $H_N(\cdot)$;

2. both UAVS are in two different edge-to-edge transition levels $H_N(\cdot)$; and

3. one UAV is on one of the ascending or descending paths and the other is on an edge-to-edge transition level $H_N(\cdot)$.

The spacing between the vertical ascending and descending paths is at least as large as the minimal spacing $d(\mathcal{A}_N)$ between the intersection points $\mathcal{A}_N$ of a node N, which in turn is larger than the acceptable conflict-free separation d_{sep} from Eq. 11. Furthermore, there can be no conflicts under the second case when both UAVs are on different levels if the edge-to-edge transition levels are separated by at least the acceptable conflict-free separation d_{sep}. Under the third case, the distance between two UAVs can become smaller than the minimal spacing $d(\mathcal{A}_N)$ between the intersection points $\mathcal{A}_N$ of a node N. For example, consider the distance between two UAVs when both are on the same edge-to-edge transition level, e.g., $H_9(2)$ from Fig. 3c, when one UAV $U(1)$ is is presently located at a_b on a vertical path and is transitioning to another level, e.g., $H_9(3)$ while the other UAV $U(2)$ is located at z_b on a transition path from location b_b on level $H_9(2)$ to the location $9b$ on the same level, above the node 9, as shown in Fig. 4.
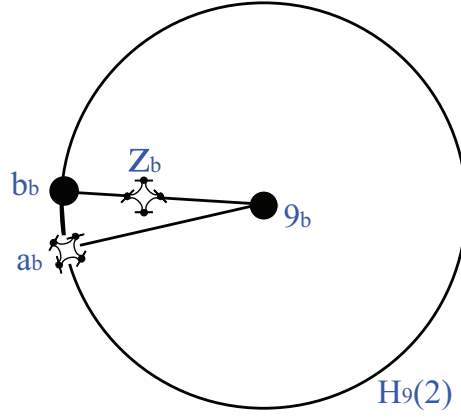
Fig. 4 Third case: one UAV is inside a level and other is changing levels.

Conflict can occur when UAV $U(1)$ is at location a_b, which is the closest that UAV $U(1)$ gets to location z_b of UAV $U(2)$, i.e., where its vertical ascent path intersects the edge-to-edge transition level $H_9(2)$. The distance $d(a_b, z_b)$ between the two UAVs $U(1)$ and $U(2)$ can be found from triangle $\Delta(z_b 9_b a_b)$ using the law of cosines as,

$$d(a_b, z_b)^2 \ = d(z_b, 9_b)^2 \ + d(a_b, 9_b)^2 \ - 2d(z_b, 9_b)d(a_b, 9_b)\cos(\angle z_b 9_b a_b) \tag{15}$$

where the distance $d(a_b, 9_b)$ is the radius $d^*[9]$ of the conflict-free boundary circle $B_c[9]$, i.e.,

$$d(a_b, 9_b) = d^*[9]. \tag{16}$$

If the angle $\angle z_b 9_b a_b$ is obtuse, then the UAVs cannot have a conflict since, from Eqs. 15, and 16,

$$
\begin{aligned}
d(a_b, z_b)^2 \ &= \ d(9_b, z_b)^2 \ + (d^*[9])^2 \ - 2d(z_b, 9_b)(d^*[9])\cos(\angle z_b 9_b a_b) \\
&\geq \ (d^*[9])^2 \quad \text{since } cos(\angle z_b 9_b a_b) \leq 0 \\
&\geq \ (d_{sep})^2 \quad \text{from Eq. 10.}
\end{aligned}
\tag{17}
$$

When the angle $\angle z_b 9_b a_b$ is not obtuse, i.e.,

$$\angle z_b 9_b a_b \ = \angle b_b 9_b a_b \ \leq \pi/2, \tag{18}$$

the distance $d(a_b, z_b)$ between the UAVs cannot be smaller than the perpendicular distance $d_\perp(a_b, \overline{b_b 9_b})$ between location a_b and line segment $\overline{b_b 9_b}$, i.e.,

$$
\begin{aligned}
d(a_b, z_b) \ \geq d_\perp(a_b, \overline{b_b 9_b}) \ &= \ d(a_b, 9_b)\sin(\angle b_b 9_b a_b) \\
&= \ d^*[9]\sqrt{1 - \cos^2(\angle b_b 9_b a_b)}.
\end{aligned}
\tag{19}
$$

14

Moreover, from the law of cosines for triangle $\Delta(b_b 9_b a_b)$,

$$
\begin{aligned}
\cos\left(\angle a_b 9_b b_b\right) &= \frac{d(b_b, 9_b)^2 + d(a_b, 9_b)^2 - d(a_b, b_b)^2}{d(b_b, 9_b) d(a_b, 9_b)} \\
&= \frac{2(d^*[9])^2 - d(a_b, b_b)^2}{2(d^*[9])^2} = 1 - \frac{d(a_b, b_b)^2}{2(d^*[9])^2}
\end{aligned} \tag{20}
$$

since distances $d(a_b, 9_b)$ and $d(b_b, 9_b)$ are equal to the radius $d^*[9]$ of the conflict-free boundary circle $B_c[9]$, i.e.,

$$
d(a_b, 9_b) = d(b_b, 9_b) = d^*[9] \tag{21}
$$

and the law of cosines for triangle $\Delta(b_b 9_b a_b)$, Eq. 18 and Eq. 21 yield,

$$
\begin{aligned}
d(a_b, b_b)^2 &= d(b_b, 9_b)^2 + d(a_b, 9_b)^2 - d(b_b, 9_b) d(a_b, 9_b) \cos(\angle b_b 9_b a_b) \\
&= 2(d^*[9])^2 - (d^*[9])^2 \cos(\angle z_b 9_b a_b) \\
&\leq 2(d^*[9])^2.
\end{aligned} \tag{22}
$$

Then, from Eqs. 19, 20 and 22, the distance between the UAVs $d(a_b, z_b)$ satisfies

$$
\begin{aligned}
d(a_b, z_b) &\geq d^*[9] \sqrt{1 - \left[1 - \frac{d(a_b, b_b)^2}{2(d^*[9])^2}\right]^2} = d(a_b, b_b) \sqrt{\left[1 - \frac{d(a_b, b_b)^2}{4(d^*[9])^2}\right]^2} \\
&\geq d(a_b, b_b) \sqrt{\left[1 - \frac{(\sqrt{2} d^*[9])^2}{4(d^*[9])^2}\right]^2} = \frac{1}{\sqrt{2}} d(a_b, b_b) \geq \frac{1}{\sqrt{2}} d(\mathcal{A}_9).
\end{aligned} \tag{23}
$$

Sufficient spacing, i.e.,

$$
d(a_b, z_b) \geq d_{sep}, \tag{24}
$$

can be ensured if the minimal distance $d(\mathcal{A}_9)$ in Eq. 23 between intersection points $\mathcal{A}_9$ of node 9 can be designed to be sufficiently large. In particular, choosing a large radius $d^*[9]$ of the conflict-free boundary circle $B_c[9]$ enables a large separation between the intersection points $\mathcal{A}_9$ that need to be distributed on the circumference of the conflict-free boundary circle $B_c[9]$, i.e., to achieve

$$
d(\mathcal{A}_9) \geq \sqrt{2}\, d_{sep} \tag{25}
$$

to ensure the condition in Eq. 24 that the distance $d(a_b, z_b)$ between the UAVs satisfies the separation requirement,

$$
d(a_b, z_b) \geq \frac{1}{\sqrt{2}} d(\mathcal{A}_9) \geq d_{sep}. \tag{26}
$$

Assumption 4 (Sufficiently-spaced intersection points) *Each node N that has more than one edge-to-edge transition, i.e., a potential for conflict during edge-to-edge transition, the minimal distance $d(\mathcal{A}_N)$ in Eq. 11 between intersection points $\mathcal{A}_N$ of node N is sufficiently large, i.e., satisfies Eq. 25. Moreover, the height $h^*[N]$ of the conflict-free boundary cylinder in Assumption 2 is sufficiently large so that the edge-to-edge transition levels $H_N(\cdot)$ are sufficiently separated ($h_N \geq d_{sep}$) to avoid conflicts between UAVs at different levels, and all levels can be contained inside the conflict-free boundary cylinder.*

Under Assumptions 1-4 there are no conflicts between UAVs in the uNet whose routes do not share an edge.

Remark 4 (Non-vertical ascent and descent) *If vertical ascent and descent is not feasible (e.g., with the inclusion of fixed-wing UAVs), then the edge-to-edge transition scheme can be modified with gradual ascent and descent. In particular, by making the size of the circles $C_N(\cdot)$ around which transition points into and out of each level are made larger for levels that are closer to the node N. For example, the circle $C_9(3)$ at level $H_9(3)$ in the example in Fig. 3, around which transition points at locations a_f, c_f and f_f are arranged, can be the smallest, followed by a larger level $H_9(2)$ and level $H_9(1)$ can be the largest, as illustrated in 5(a). It is also possible to consider bounded turn rates, e.g., as studied in [51], which can require the use of increased spacing and smoother turns rather than sharp turns to ensure safety.*

Remark 5 (Narrow streets) *In narrow streets, for sufficient separation between edges, only one edge might be permitted, unless the UAVs fly above the buildings. Alternatively, two edges could be stacked vertically one above the other to enable flight in two directions, In this case the arrivals can be separated into different levels, and the proposed approach can be used to ascend or descend to a different edge, as illustrated in Fig. 5(b).*

Remark 6 (On-demand de-confliction) *The vertical ascent and descent adds time to the UAV flight. It is possible to only use the different levels when needed, e.g., as in on-demand de-conflicting schemes [52]. For example, if there are no conflicts at a node N for the kth UAV $U(k)$ with previously scheduled UAVs, then the UAV $U(k)$ can directly proceed from the intersection point $\underline{a}_N(\cdot)$ into the*

node at the circumference of the conflict-free boundary circle $B_c[N]$ to node N followed by movement to the intersection point $\bar{a}_N(\cdot)$ out of the node N. If there is potential for conflict, say for UAV $U(k+1)$ with UAV $U(k)$, then the later UAV $U(k+1)$ selects the next-closest available level $H_N(\cdot)$ to achieve the edge-to-edge transition, as illustrated in Fig. 5(c).

(a) Non-vertical ascent & descent   (b) Arrival & departure at different level   (c) On-demand de-conflicting
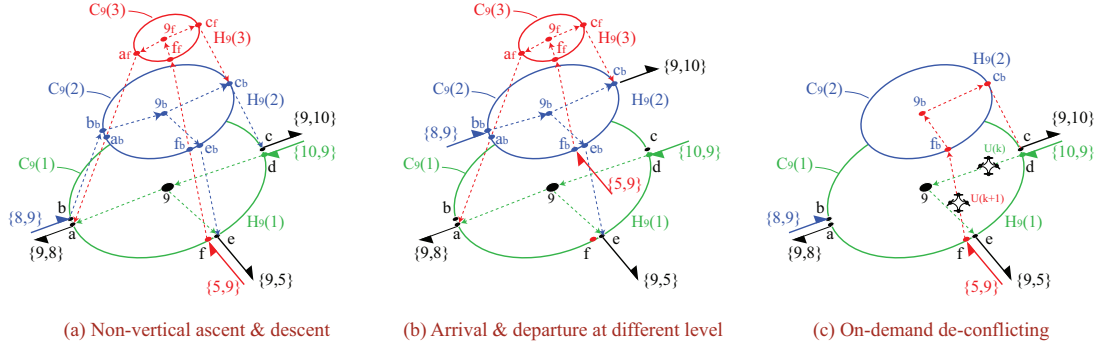
Fig. 5 Schematic alternate approaches to decoupling edge-to-edge transitions at node 9**.**

B. Scenario 2: de-conflicting UAV routes with shared edge

The second scenario for potential conflict occurs between UAVs on routes that share an edge. There are two conflict cases under this scenario: (i) during turns when UAVs are following each other; and (ii) during merges into an edge.

1. Case 1: de-conflicted turns when UAVs follow each other

The first case of conflicts during turns is studied here. Note that even if two UAVs on a single edge are sufficiently separated initially, the spacing between them can decrease when making turns, e.g., for making edge-to-edge transitions at a node or on turns within a single edge. Therefore, the spacing between UAVs following each other on a turn edge needs to be sufficiently large to ensure conflict-free turns as shown in previous works for conflict resolution, e.g., [43, 52]. In particular, if two UAVs have the same speed V (m/s) on an edge, then two UAVs arriving on the edge, one following the other, are conflict-free during turns on the edge if they are separated in arrival time

at the start of the edge by minimal time T_{min} that satisfies, e.g., see Lemma 2 in [43],

$$T_{min} = \frac{1}{V} d_{min} = \frac{1}{V} \left[\frac{d_{sep}}{\cos(\phi^*/2)} \right] \qquad (27)$$

where $\phi^* < \pi$ is the maximum turn angle between straight sections of the route and d_{min} is the minimal separation between UAVs along straight sections of the route, as shown in Fig. 6. This is formally stated in the following assumption.
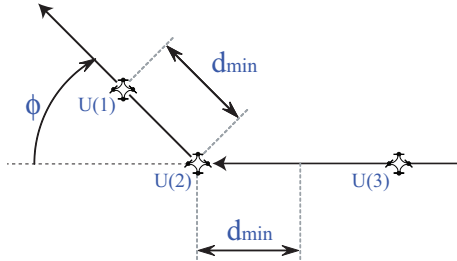
Fig. 6 Increased spacing needed (d_{min} in Eq. 27) for heading change ϕ.

Assumption 5 (Constant-speed flight) *The edges and transitions between the edges are considered to be straight segments and turn between these segments of angle ϕ less than the maximum turn angle of ϕ^*. The speed of UAVs along all straight sections in the route network is a constant V m/s and scheduled time of arrivals (STAs) into each input location $L_i(\cdot)$ in the route network will be spaced at least by the minimal time T_{min} for conflict-free turns in Eq. 27. Moreover, the height $h^*[N]$ of the conflict-free boundary cylinder in Assumption 2 is sufficiently large so that the edge-to-edge transition levels $H_N(\cdot)$ are sufficiently separated*

$$h_N \geq d_{min} \qquad (28)$$

to decouple potential conflicts due to multiple heading changes at different levels [43], and all levels can be contained inside the conflict-free boundary cylinder.

Remark 7 (UAVs with different speeds) *The spacing condition in Eq. 27 for conflict-free turns can be generalized to include UAVs with different speeds and turn dynamics, e.g., see spacing conditions developed in [51, 53]. If the UAVs have several substantially different operating speeds, then it might be advantageous to create a different set of routes for each operating speed. Other*

solutions, e.g., with variable speed UAVs, could include waiting for sufficient time just before arriving at each node to avoid conflicts with UAVs passing through the node that were scheduled earlier. However, the resulting wait-related delay could be avoided by the proposed de-conflicting approach using out-of-plane edge-to-edge transitions.

2. Case 2: de-conflicted merging into a shared edge

A scheduling-based de-conflicting approach for the second case in the shared-edge scenario, i.e., for conflicts between UAVs merging into a shared edge, is studied next. Consider two UAVs, say $U(1)$ and $U(2)$ transition from two different edges, say $\underline{E}_N(1)$ and $\underline{E}_N(2)$, in the set of edges $\underline{\mathcal{E}}_N$ into node N to the same edge, say $\overline{E}_N(3) \in \overline{\mathcal{E}}_N$, out of node N. Then, there is potential for conflict at the intersection point $\overline{a}_N(3)$ of the edge $\overline{E}_N(3)$ with the the conflict-free boundary circle $B_c[N]$. For example, consider two UAVs $U(1)$ and $U(2)$ transitioning from two different edges $\underline{E}_9(1) = \{10, 9\}$ and $\underline{E}_9(2) = \{8, 9\}$ into node $N = 9$ to the same edge $\overline{E}_9(3) = \{9, 5\}$ out of node $N = 9$. Then, there is potential for conflict at the intersection $\overline{a}_9(3) = e$ of the output edge $\overline{E}_9(3)$ with the conflict-free boundary circle $B_c[9]$, as in Fig. 7. In particular, conflict occurs if both UAVs $U(1)$ and $U(2)$ attempt to reach the location e at the same time. Conflict can be avoided if the arrival times $t_e(1)$ and $t_e(2)$ for the two UAVs $U(1)$ and $U(2)$, respectively, at location e of the edge $\{9, 5\}$ out of the node 9 are sufficiently separated, i.e.,

$$|t_e(1) - t_e(2)| \;\; > \;\; d_{min}/V \;\; = \;\; T_{min}. \tag{29}$$
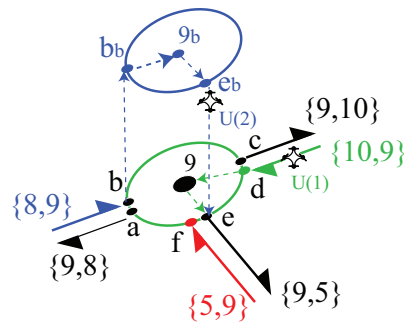
Fig. 7 Potential conflict at e when UAVs $U(1)$ and $U(2)$ merge into edge $\{9, 5\}$.

Remark 8 (Sufficency of de-conflicting at arrival points) *Since the UAVs have the same travel speed V from Assumption 5, the spacing of arrivals of UAVs by the minimum time T_{min} at any intersection point of an edge out of a node N with its conflict-free boundary circle $B_c[N]$ ensures that the UAVs remain separated, both before and after, as long as they continue to travel together along the same set of edges and nodes.*

Assumption 6 (Isolation from UAVs outside uNet) *The uNet is sufficiently isolated and there are are no conflicts with UAVs in the uNet and other UAVs outside of the uNet, e.g., with UAVs prior to its arrival into the uNet at an intersection point in the set $\mathcal{A}_{L_i(k)}$ associated with node $L_i(k)$ and after its final departure from the UAV from an intersection point in the set $\mathcal{A}_{L_f(k)}$ associated with node $L_f(k)$.*

At each intersection point $a_N(i) \in \mathcal{A}_N$ of edges associated with node N and its conflict-free boundary circle $B_c[N]$, let the associated UAV arrival times be $t_{a_N(i)}(k)$ such that $t_{a_N(i)}(k) < t_{a_N(i)}(k+1)$ for $k < k+1$. Then, under Assumptions 1-6 and with the proposed de-conflicting scheme, there are no conflicts provided the arrival times of UAVs $t_{a_N(i)}(k)$ (at each intersection point $a_N(i)$ of each node N) are sufficiently separated, i.e.,

$$t_{a_N(i)}(k+1) - t_{a_N(i)}(k) \quad > T_{min}. \tag{30}$$

Remark 9 (Managing uncertainties) *The proposed approach relies on UAVs meeting scheduled arrival times at different nodes. If a scheduled arrival time is not met, then the spacing between the UAVs could become lower than the minimal spacing d_{sep}. One approach to manage small uncertainties in the arrival time is to provide some additional buffer, i.e., by using a larger minimal spacing d_{sep} in the uNet design, e.g., as in [43]. Additionally, the operating speed of UAVs in the uNet should be below the maximum operating speed of the UAVs, to enable short-duration increases in speeds to meet a specified arrival time at the next node.*

IV. Example conflict-free UAV scheduling

The separation of arrival times at the intersection points $\mathcal{A} = \bigcup_N \mathcal{A}_N$ of edges and conflict-free boundary circle $B_c[N]$ of each node N of the route network can be achieved using existing solutions

to resource allocation problems. Scheduling for the proposed uNet is illustrated with the context-aware route planning (CARP), where a new agent selects a route and schedules the arrival time such that the new agent is conflict-free with respect to previous agents [44].

A. Example uNet

Consider an example uNet, shown in Fig. 8. This is an an lllustrative example that includes multiple sectors and the typical intersection types. The example does have the advantage of simplicity and sufficient details are provided for potential comparative evaluations with other methods that might be developed in the future. It is composed of four repetitions of the sNet $S(1)$ in Fig. 2, where the boundaries the sNets are denoted by red dashed lines in Fig. 8. Potential initial and final node locations L_i and L_f, respectively, are to be selected from the set $\mathcal{L}$

$$\mathcal{L} = \{1, 2, 3, 7, 13, 14, 17, 20, 23, 24, 28, 33, 34, 37, 40, 42\} \tag{31}$$

depicted by white circles in Fig. 8. The grid spacing of the route network in Fig. 8 is assumed to be 100m, which is a medium-sized city block, e.g., in Seattle [54]. Since GPS with Wide Area Augmentation System (WAAS) can have positioning error of say $3 - 7$m, ideally the minimal separation d_{sep} between UAVs should be $6 - 14$m. Given the five edge intersection at, say node 4, de-conflicting the edge-to-edge transitions would require a separation of the UAV path into four paths at each level, e.g., as in Fig. 3. On-demand de-confliction as in Remark 6, e.g., to only use the different levels when needed, is not considered here. Assuming that all the paths are uniformly distributed, i.e., at angle $2\pi/5$ from each other, this requires a maximum heading change of $\phi^* = \pi - 2\pi/5 = 3\pi/5$. Then the minimal separation between the UAVs is $d_{min} = d_{sep}/cos(\phi^*/2) = 10 - 23$m from Eq. 27. The spacing between UAVs on the same route is assumed to be $d_{min} = 20$m. With a speed of say $V = 4$m/s (about a tenth of the maximum expected UAV speed [55]), the time spacing T_{min} between UAV arrivals then needs to be $T_{min} = d_{min}/V = 5$s.

B. Selection of UAV arrivals into uNet

Simulations were performed to assess delays with the proposed FCFS scheduling approach. Note that the time needed to move across the eight grids of the example uNet in Fig. 8, with grid spacing of 100m and speed $V = 4$m/s is $T_8 = 25$s. Updates of the uNet, i.e., when new UAVs are allowed
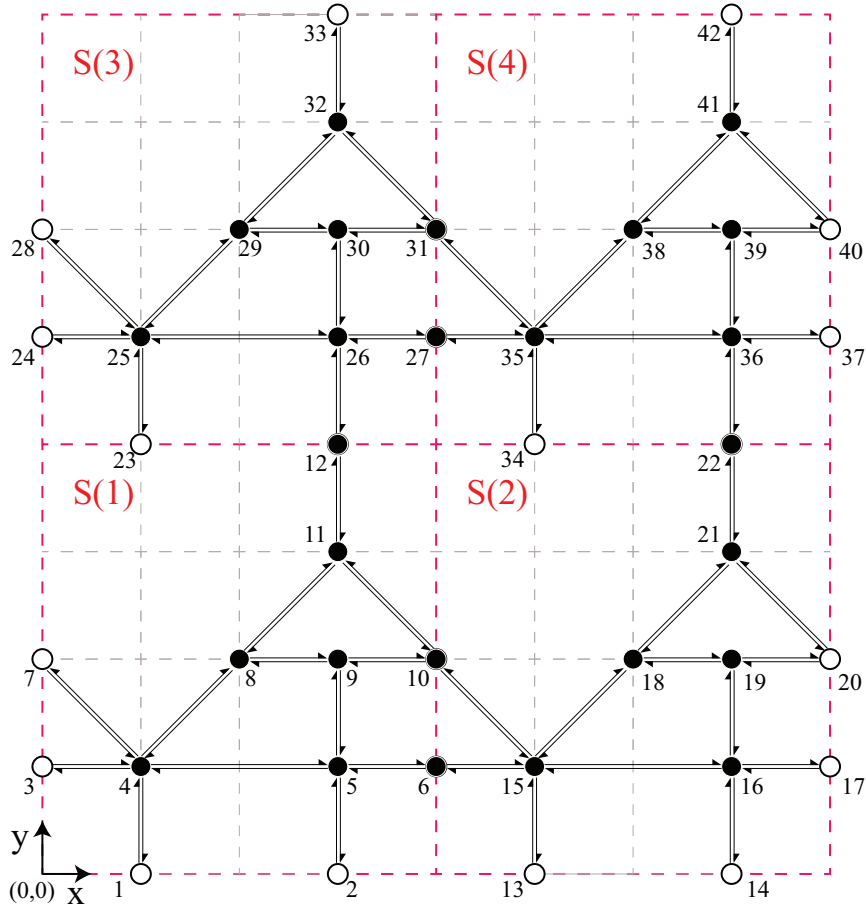
Fig. 8 Example uNet. Potential initial and final locations are depicted by white circles.

to enter were performed at a time interval of $T_\Delta = 1\text{s}$ and time t was discretized as

$$t[n] = n * T_\Delta. \tag{32}$$

Let a set of scheduled routes $R(i)$, $i = 1, 2, \cdots, k-1$ be given at discretized time instant $t[n]$. Then a random number $r[n] \in [0, 1]$ was selected and a new UAV $U(k)$ was selected with an expected time of arrival $ETA(k) = t[n]$ if the random number was less than a probability of arrival p_a, i.e.,

$$r[n] \leq p_a. \tag{33}$$

The input location $L_i(k)$ and the final location $L_f(k)$ for the UAV $U(k)$ were chosen randomly from the set $\mathcal{L}$. Then, the scheduled time of arrival $STA(k)$ was found in a two step procedure: (i) select a minimal distance route $\mathcal{R}(k)$ from the input location $L_i(k)$ to the final location $L_f(k)$ through

the network; and (ii) select a conflict-free scheduled time of arrival $STA(k)$

$$STA(k) \geq ETA(k), \tag{34}$$

that is closest to the expected time of arrival $ETA(k)$ as follows.

1. Select the scheduled time of arrival STA for UAV $U(k)$ to be the expected time of arrival $ETA(k)$.

2. Check for conflicts for UAV $U(k)$ with previously scheduled UAVs.

3. If there is a conflict in step 2, then increment the scheduled time of arrival STA by T_Δ and repeat step 2.

4. If there are no conflicts in step 2, then assign the current scheduled time of arrival STA to UAV $U(k)$.

The process of generating a random number at update time $t[n]$ was repeated, e.g., for UAV $U(k+1)$ until the random number was larger than the probability of a UAV arrival, i.e., $r[n] > p_a$ resulting in no new UAVs. The update time was then incremented to $t[n+1]$. Note that more than one UAV can have an expected time of arrival ETA of $t[n]$. The process was stopped when the number of UAVs in the system reached $k = 1000$.

C. Simulation results

The delay $D(k) = STA(k) - ETA(k)$ for each UAV was found and is plotted as a function of the probability p_a in Fig. 9 for a 1000 UAVs. Seven simulation trials were done for each different arrival probability p_a. The simulations results are shown for two different arrival time separations T_{min} were used: left plot, $T_{min} = 5$s; and right plot, $T_{min} = 2$s. In these simulations, the time of flight from the departure intersection point in $\mathcal{A}_N(i)$ of a node $N(i)$ to the arrival intersection point in $\mathcal{A}_N(j)$ of another node $N(j)$ was approximated by the distance between the two nodes. As expected, the delays tend to increase with probability of arrival p_a. Delays can be reduced by using a smaller arrival time separation, e.g. for $T_{min} = 2$s instead of for $T_{min} = 5$s, as seen in Fig. 9. The average maximum delay, e.g., for arrival probability $p_a = 0.5$ decreases by 87.3%, from 97.6s to 12.4s when the separation time is decreased from $T_{min} = 5$s to $T_{min} = 2$s.
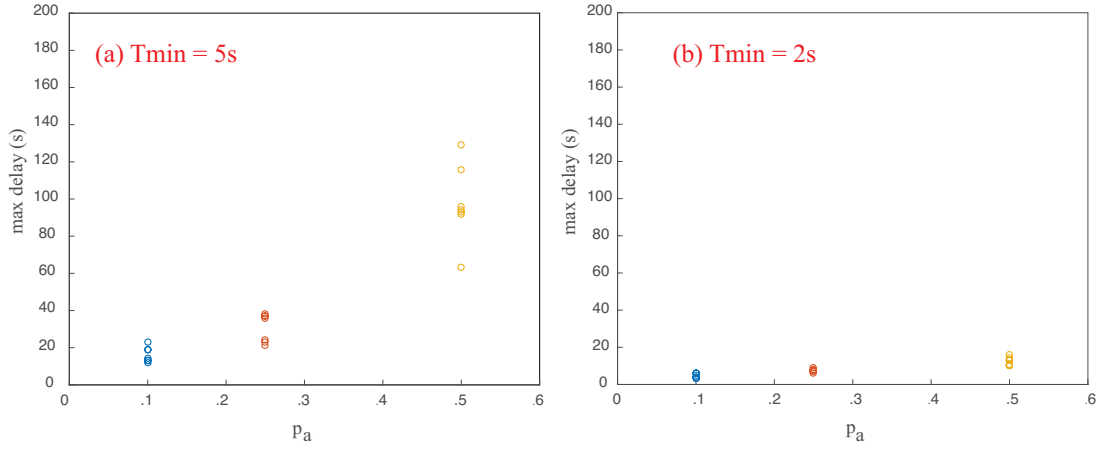
Fig. 9 Delays for different arrival probability p_a and arrival time separation T_{min}.

Substantial delays might not be acceptable to users. The simulation results indicate the effect of potential UAV conflict (e.g., the separation requirement) on delays. As the UAV density increases, or as the separation requirements get large, there can be a substantial impact on the delays in the system. Clearly, one approach to reduce delays is to increase precision of the UAV navigation system, i.e., decrease the arrival time spacing T_{min} between UAVs, however, this can increase costs. An alternative approach is to choose a set of possible routes $\mathcal{R}(k)$ consisting of more than one viable route for each UAV. Then, an optimal route $R(k) \in \mathcal{R}(k)$ can be selected to optimize other criteria such as minimal delay between expected time of arrival at the destination $ETA_d(k)$ and scheduled time of arrival at the destination $STA_d(k)$. Note that a longer route (not energy optimal) might lead to a smaller delay at the destination. Other combinations of the energy cost (path length that can be approximated by $STA_d(k) - STA(k)$) and the delay at the destination $STA_d(k) - ETA_d(k)$ can be used to select a route $R(k)$ from the set of acceptable routes $\mathcal{R}(k)$. Another approach to reduce delays is to modify the route network. If certain routes have high demand, additional routes could be added in parallel to these dense route or allow UAVs to bypass the congested areas. Similarly, direct higher-speed edges could be added between very high demand nodes to reduce the overall delay in the system.

D. Future work

The implementation of the proposed uNet approach will require additional development and evaluation of protocols for emergencies. For example, an evaluation of the proposed uNet approach for human factors issues is needed to ensure that human supervisors can monitor and maintain overall situational awareness of overall system. The scheduling approach can be extended to accommodate human-operated systems in the uNet route structure provided the intended route is known. Additionally, if the UAV is not able to reach intermediate nodes in a specified time, e.g., due to uncertainties such as wind, routing is needed to land the UAV in a designated location, or the routing needs to be dynamically updated. Such emergency re-routing could be a pre-planned set of waypoints specific to each edge section in the route network. Moreover, sensors on-board the UAV could also check for battery life with planned stops for battery swaps for long-distance travel. Moreover, to ensure that the UAVs can meet the uNet requirements, certification protocols need to be established and testing facilities are needed to prove UAV viability before acceptance into the uNet. Such viability tests could include the ability of the UAV to obtain GPS data, communicate with a typical sNet, and power usage to assess range of operation. Finally, as with self-driving cars, risk assessment and liability issues will need to be addressed to handle situations such as a UAV crash on a roadway. Future work could also study strategies such as reducing the number of UAVs in the uNet to manage large scale changes in the operating conditions, e.g., as in conventional air-traffic flow management [56].

V. Conclusions

This article proposed a new Unmanned Aerial Vehicle (UAV) operation paradigm to enable a large number of relatively low-cost UAVs to fly beyond-line-of-sight. The use of an established route network for UAV traffic management was proposed to reduce the onboard sensing requirements for avoiding such obstacles and enable the use of of well-developed routing algorithms to select UAV schedules that avoid conflicts. Another contribution of this work was to propose a decoupling scheme for conflict-free transitions between edges of the route network at each node to reduce potential conflicts between UAVs and ensuing delays. A simulation example and an example first-

come-first-served scheduling scheme was used to illustrate the uNet approach.

[1] E. Frazzoli, Z.-H. Mao, J.-H. Oh, and E. Feron. Resolution of conflicts involving many aircraft via semidefinite programming. *Journal of Guidance, Control, and Dynamics*, 24(1):79–86, 2001.

[2] L. Pallottino, E. M. Feron, and A. Bicchi. Conflict resolution problems for air traffic management systems solved with mixed integer programming. *IEEE Trans. Intel. Trans. Sys.*, 3(1):3–11, Mar. 2002.

[3] D.K. Schmidt. On modelling ATC workload and sector capacity. *J. of Aircraft*, 13(7), Jul 1976.

[4] Milan Jani*ć*. A model of air traffic control sector capacity based on air traffic controller workload. *Transportation Planning and Technology*, 20(4):311–335, 1997.

[5] H. Erzberger. Design principles and algorithms for automated air traffic management. *AGARD Lecture Series No. 200, Knowledge-Based Functions in Aerospace Systems, San Francisco*, November, 1995.

[6] Caitlin Ailis Kenny. Unmanned Aircraft System (UAS) Delegation of Separation in NextGen Airspace. Master's thesis, San Jose State University, San Jose, CA, 2013.

[7] Andrew Lacher, Andrew Zeitlin, David Maroney, Kelly Markin, Duane Ludwig, and Joe Boyd. Airspace integration alternatives for unmanned aircraft. *Proc. of the AUVSI Unmanned Systems Asia-Pacific 2010, Pan Pacific Hotel, Singapore*, pages 1–19, 1 Feb 2010 2010.

[8] Ling Qiu, Wen-Jing Hsu, Shell-Ying Huang, and Han Wang. Scheduling and routing algorithms for agvs: a survey. *International Journal of Production Research*, 40(3):745–760, 2002.

[9] N. Smolic-Rocak, S. Bogdan, Z. Kovacic, and T. Petrovic. Time windows based dynamic routing in multi-agv systems. *Automation Science and Engineering, IEEE Transactions on*, 7(1):151–155, Jan 2010.

[10] S. Devasia and G. Meyer. Automated conflict resolution procedures for air traffic management. *Proceedings of the 36th Conference on Decision and Control, Phoenix, AZ*, pages 2456–2462, December 1999.

[11] E. Besada-Portas, L. de la Torre, J. M. de la Cruz, and B. Andres-Toro. Evolutionary trajectory planner for multiple uavs in realistic scenarios. *IEEE Transactions on Robotics*, 26(4):619–634, Aug., 2010.

[12] Peng Yang, Ke Tang, Jose A. Lozano, and Xianbin Cao. Path planning for single unmanned aerial vehicle by separately evolving waypoints. *IEEE Transactions on Robotics*, 31(5):1130–1146, October 2011.

[13] Am Cho, Jihoon Kim, Sanghyo Lee, Sujin Choi, Boram Lee, Bosung Kim, Noha Park, Dongkeon Kim, and Changdon Kee. Fully automatic taxiing, takeoff and landing of a uav using a single-antenna gps receiver only. In *International Conference on Control, Automation and Systems, 2007. ICCAS '07,*

pages 821–825, Oct 2007.

[14] Thomas W. Carnes. A low cost implementation of autonomous takeoff and landing for a fixed wing UAV. Master's thesis, Virginia Commonwealth University, Richmond, Virginia, 2014.

[15] S. Devasia, D. Iamratanakul, G. Chatterji, and G. Meyer. Decoupled conflict-resolution procedures for decentralized air traffic control. *IEEE Trans. on Intelligent Transportation Systems*, 12(2):422–437, June 2011.

[16] Adriaan W. ter Mors, Cees Witteveen, Jonne Zutt, and Fernando A. Kuipers. Context-aware route planning. In Jürgen Dix and Cees Witteveen, editors, *Multiagent System Technologies*, volume 6251 of *Lecture Notes in Computer Science*, pages 138–149. Springer Berlin Heidelberg, 2010.

[17] D. Bertsimas and S. S. Patterson. The traffic flow management rerouting problem in air traffic control: A dynamic network flow approach. *Transportation Science*, 34(3):239–255, Aug., 2000.

[18] Steven L. Waslander, Robin L. Raffard, and Claire J. Tomlin. Toward efficient and equitable distributed air traffic flow control. *Proc. of the American Control Conference, Minneapolis, Minnesota, USA, June 14-16, 2006*, pages 5189–5194, 2006.

[19] Avijit Mukherjee and Mark Hansen. A dynamic rerouting model for air traffic flow management. *Transportation Research Part B*, 43(1):159–171, 2009.

[20] Cyril Allignol, Nicolas Barnier, Pierre Flener, and Justin Pearson. Constraint programming for air traffic management : a survey. *The Knowledge Engineering Review, Elsevier*, 27(3):361–392, 2012.

[21] Jin Y. Yen. Finding the k shortest loopless paths in a network. *Management Science*, 17(11):712–716, July 1971.

[22] Jonathan D. Stevenson, Siu O'Young, and Luc Rolland. Beyond line of sight control of small unmanned aerial vehicles using a synthetic environment to augment first person video. *Procedia Manufacturing*, 3:960–967, 2015.

[23] J. Yoo and S. Devasia. Provably safe conflict resolution with bounded turn rate for air traffic control. *IEEE Trans. on Control Systems Technology*, 21(6):2280–2289, November 2013.

[24] J. Yoo and S. Devasia. On-demand conflict resolution procedures for air traffic intersections. *IEEE Trans. on Intelligent Transportation Systems*, 15(4):538–1549, August 2014.

[25] J. D. Yoo and S. Devasia. Decoupled conflict resolution procedures for non-perpendicular air traffic intersections with different speeds. *52nd IEEE Annual Conference on Decision and Control (CDC), Florence, Italy*, pages 275–280, December, 10-13 2013.

[26] Arnis Siksna. The effects of block size and form in North American and Australian city centers. *Urban Morphology*, 1, ISSN 1027-4278:19–33, 1997.

[27] Federal Aviation Administration. Operation and certification of small unmanned aircraft systems. *Docket No.: FAA-2015-0150; Notice No. 15-01, RIN 2120-AJ60*, February 15, 2015.

[28] Y. Wan and S. Roy. A scalable methodology for evaluating and designing coordinated air-traffic flow management strategies under uncertainty. *IEEE Trans. Intel. Trans. Sys.*, 9(4):644–656, Dec. 2008.

[29] E. Frazzoli, Z.-H. Mao, J.-H. Oh, and E. Feron. Resolution of conflicts involving many aircraft via semidefinite programming. *Journal of Guidance, Control, and Dynamics*, 24(1):79–86, 2001.

[30] L. Pallottino, E. M. Feron, and A. Bicchi. Conflict resolution problems for air traffic management systems solved with mixed integer programming. *IEEE Trans. Intel. Trans. Sys.*, 3(1):3–11, Mar. 2002.

[31] D.K. Schmidt. On modelling ATC workload and sector capacity. *J. of Aircraft*, 13(7), Jul 1976.

[32] Milan Janić. A model of air traffic control sector capacity based on air traffic controller workload. *Transportation Planning and Technology*, 20(4):311–335, 1997.

[33] H. Erzberger. Design principles and algorithms for automated air traffic management. *AGARD Lecture Series No. 200, Knowledge-Based Functions in Aerospace Systems, San Francisco*, November, 1995.

[34] Caitlin Ailis Kenny. Unmanned Aircraft System (UAS) Delegation of Separation in NextGen Airspace. Master's thesis, San Jose State University, San Jose, CA, 2013.

[35] Andrew Lacher, Andrew Zeitlin, David Maroney, Kelly Markin, Duane Ludwig, and Joe Boyd. Airspace integration alternatives for unmanned aircraft. *Proc. of the AUVSI Unmanned Systems Asia-Pacific 2010, Pan Pacific Hotel, Singapore*, pages 1–19, 1 Feb 2010 2010.

[36] Ling Qiu, Wen-Jing Hsu, Shell-Ying Huang, and Han Wang. Scheduling and routing algorithms for agvs: a survey. *International Journal of Production Research*, 40(3):745–760, 2002.

[37] N. Smolic-Rocak, S. Bogdan, Z. Kovacic, and T. Petrovic. Time windows based dynamic routing in multi-agv systems. *Automation Science and Engineering, IEEE Transactions on*, 7(1):151–155, Jan 2010.

[38] S. Devasia and G. Meyer. Automated conflict resolution procedures for air traffic management. *Proceedings of the 36th Conference on Decision and Control, Phoenix, AZ*, pages 2456–2462, December 1999.

[39] E. Besada-Portas, L. de la Torre, J. M. de la Cruz, and B. Andres-Toro. Evolutionary trajectory planner for multiple uavs in realistic scenarios. *IEEE Transactions on Robotics*, 26(4):619–634, Aug., 2010.

[40] Peng Yang, Ke Tang, Jose A. Lozano, and Xianbin Cao. Path planning for single unmanned aerial vehicle by separately evolving waypoints. *IEEE Transactions on Robotics*, 31(5):1130–1146, October 2011.

[41] Am Cho, Jihoon Kim, Sanghyo Lee, Sujin Choi, Boram Lee, Bosung Kim, Noha Park, Dongkeon Kim, and Changdon Kee. Fully automatic taxiing, takeoff and landing of a uav using a single-antenna gps receiver only. In *International Conference on Control, Automation and Systems, 2007. ICCAS '07*, pages 821–825, Oct 2007.

[42] Thomas W. Carnes. A low cost implementation of autonomous takeoff and landing for a fixed wing UAV. Master's thesis, Virginia Commonwealth University, Richmond, Virginia, 2014.

[43] S. Devasia, D. Iamratanakul, G. Chatterji, and G. Meyer. Decoupled conflict-resolution procedures for decentralized air traffic control. *IEEE Trans. on Intelligent Transportation Systems*, 12(2):422–437, June 2011.

[44] Adriaan W. ter Mors, Cees Witteveen, Jonne Zutt, and Fernando A. Kuipers. Context-aware route planning. In Jürgen Dix and Cees Witteveen, editors, *Multiagent System Technologies*, volume 6251 of *Lecture Notes in Computer Science*, pages 138–149. Springer Berlin Heidelberg, 2010.

[45] D. Bertsimas and S. S. Patterson. The traffic flow management rerouting problem in air traffic control: A dynamic network flow approach. *Transportation Science*, 34(3):239–255, Aug., 2000.

[46] Steven L. Waslander, Robin L. Raffard, and Claire J. Tomlin. Toward efficient and equitable distributed air traffic flow control. *Proc. of the American Control Conference, Minneapolis, Minnesota, USA, June 14-16, 2006*, pages 5189–5194, 2006.

[47] Avijit Mukherjee and Mark Hansen. A dynamic rerouting model for air traffic flow management. *Transportation Research Part B*, 43(1):159–171, 2009.

[48] Cyril Allignol, Nicolas Barnier, Pierre Flener, and Justin Pearson. Constraint programming for air traffic management : a survey. *The Knowledge Engineering Review, Elsevier*, 27(3):361–392, 2012.

[49] Jin Y. Yen. Finding the k shortest loopless paths in a network. *Management Science*, 17(11):712–716, July 1971.

[50] Jonathan D. Stevenson, Siu O'Young, and Luc Rolland. Beyond line of sight control of small unmanned aerial vehicles using a synthetic environment to augment first person video. *Procedia Manufacturing*, 3:960–967, 2015.

[51] J. Yoo and S. Devasia. Provably safe conflict resolution with bounded turn rate for air traffic control. *IEEE Trans. on Control Systems Technology*, 21(6):2280–2289, November 2013.

[52] J. Yoo and S. Devasia. On-demand conflict resolution procedures for air traffic intersections. *IEEE Trans. on Intelligent Transportation Systems*, 15(4):538–1549, August 2014.

[53] J. D. Yoo and S. Devasia. Decoupled conflict resolution procedures for non-perpendicular air traffic intersections with different speeds. *52nd IEEE Annual Conference on Decision and Control (CDC),*

Florence, Italy, pages 275–280, December, 10-13 2013.

[54] Arnis Siksna. The effects of block size and form in North American and Australian city centers. *Urban Morphology*, 1, ISSN 1027-4278:19–33, 1997.

[55] Federal Aviation Administration. Operation and certification of small unmanned aircraft systems. *Docket No.: FAA-2015-0150; Notice No. 15-01, RIN 2120-AJ60*, February 15, 2015.

[56] Y. Wan and S. Roy. A scalable methodology for evaluating and designing coordinated air-traffic flow management strategies under uncertainty. *IEEE Trans. Intel. Trans. Sys.*, 9(4):644–656, Dec. 2008.